The 11th International Conference on Power Electronics - ICPE - ECCE Asia

On Features of Direct Current Transformers

R. P. Barcelos and D. Dujic

POWER ELECTRONICS LABORATORY
ÉCOLE POLYTECHNIQUE FÉDÉRALE DE LAUSANNE

On Features of Direct Current Transformers

Renan Pillon Barcelos ,Dražen Dujić

Power Electronics Laboratory - PEL
École Polytechnique Fédérale de Lausanne - EPFL
Lausanne, Switzerland
renan.pillonbarcelos@epfl.ch, drazen.dujic@epfl.ch

Abstract—**The open loop operation of the DC transformer requires some intelligence to deal with the system's dynamics and transients. This converter is realized with a bidirectional LLC converter operating close to the resonant frequency and does not receive any voltage or power set points for its operation. This paper presents the required features to enable a safe and autonomous operation. Essentially, DC transformer behaves as an AC transformer, allowing the natural power flow between two dc buses, creating advanced dc grid layouts. Hence, features such as a power reversal algorithm for bidirectional operation, idle mode for the no-load condition, and soft-start and protection are some of the essential features required for its operation. Developed strategies are verified by means of experimental investigations with two similar prototypes evaluating the performance of the strategies and the difference between both DC transformers with the same features.**

Index Terms—**DC Transformer, DC Power Distribution Networks, LLC, Power Reversal, Resonant Converter.**

I. INTRODUCTION

The development of an open-loop Direct Current Transformer (DCT) is fundamental to create more advanced dc power distribution networks (PDN) in the future. Differently from point-to-point connection and multi terminals dc systems, the DCT technology can integrate DC buses of different voltages level and at the same time enable a DC network suitable to connect renewable generation and storage systems.

A well-suited topology for the DCT is the resonant LLC converter operating close to the resonant frequency. Some of the advantages are the stiff voltage ratio with a natural power flow, the dc grid isolation via medium frequency transformer (MFT), and the high efficiency due to the soft switching. Yet, the power stage connected to each dc port operates individually and does not require any synchronization or signal feedback between them. This means that while one side is switching, other side can operate as a passive rectifier, requiring only one PWM reference for the DCT.

Besides that, as a bidirectional converter, the DCT requires a power reversal detection algorithm to identify which power stage should be active. This feature is usually implemented with Power Reversal Methods (PRM) manipulating the PWM generation of the DCT. Essentially, the PRMs use current and voltage measurements to determine which power stage should be switching in order to guide the current, and in case of power reversal, the PRM block detects the change and set a command to alternate the active power stage. This feature of DCT is extensively investigated in [1].

Nonetheless, as an open-loop converter, the DCT does not have naturally any criteria to set its operating limits; only the protection limits. For a DCT operating in a DC PDN, many cases of overload and no-load can happen, and an action from the DCT may be required. For example, in the case of overload, the current would rise and the DCT would be forced to turn off for safety reasons. On the other hand, in the case of no load condition, the DCT will consume power to supply the magnetizing circuit of MFT, creating extra losses while the DCT is not operating according to the system's demand. Recognizing these conditions is important, so that adequate response of DCT can be implemented.

In literature, the overload problem is addressed by means of change to power hardware [2]–[4], and control software [5]–[9]. The solutions based on hardware propose the addition of snubber [3] for the resonant capacitor, or extra elements in the resonant tank [4]. Although this solution can solve the problem, the addition of these elements increases the volume and cost of the DCT.

The solutions based on control software can be separated into two main approaches; i) changing the switching frequency, and ii) altering the duty cycle. The first type alters the switching frequency in order to change the converter gain. However, by doing this, during heavy overload the converter would have to operate with several times the nominal switching frequency, making this technique not suitable for many switching devices [8]. The second solution alters the duty cycle, generating a three-level waveform in the resonant tank. However, this waveform in the resonant tank can increase the losses of the power stages, and extra protection should be carried out in the case of very long overload situations. In [9] the thermal protection of DCT was developed for this situation and such a strategy solves the problem of overload operation limits.

For the case of the no-load condition, the LLC converter is usually analyzed from the point of view of output voltage regulation [10], or design of LLC converter in light load conditions [11]. However, the interest of the DCT is to take advantage of no-load conditions and minimize the losses as no power is been transmitted between buses. Therefore, once the no-load condition is met, the DCT could turn off and wait for the required DC PDN conditions to start its operation again.

In summary, all the previously discussed logic blocks are essential intelligence for the operation of the DCT. These blocks need to be integrated with the PWM to complete the
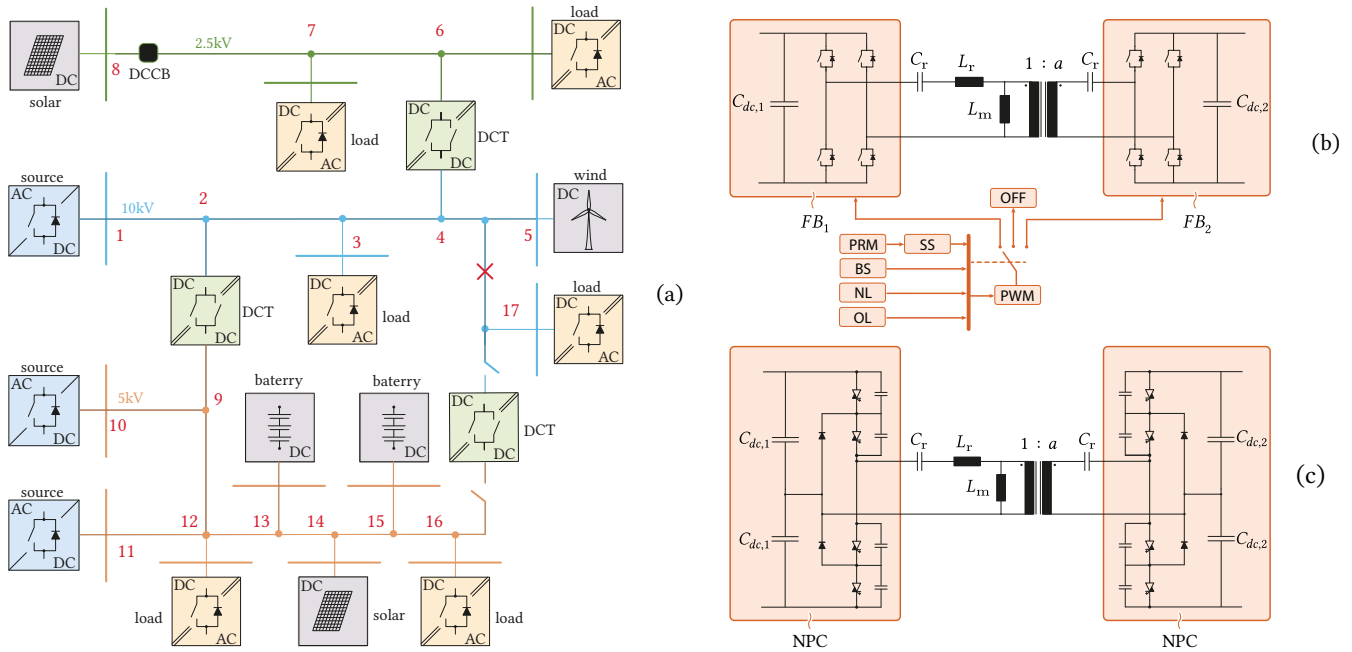
Fig. 1. (a) Illustrative example of a DC PDN with 17 nodes and 3 different voltage levels interconnected by DCTs. (b) DCT with full-bridge power stages and essential features to enable open loop operation acting in the PWM block; (c) Medium voltage DCT with NPC power stages.

DCT operation. Thus, this paper investigates these essential features and tests them in two different DCTs, evaluating their performance and the differences when using different DCTs. This paper proceeds as follows: Section II describes the DCTs under analysis, with the DC PDN and cases of study. In Section III the power reversal methods and no-load conditions are presented, followed by Section IV with experimental results and comparison. In Section V, a discussion about the autonomous operation of DCT is presented, and in Section VI the conclusions.

II. DC PDN AND DCT TOPOLOGY

An illustrative example of a DC PDN with several DCTs is shown in Fig. 1a. For this system, the AC-DC converters control the voltage of each bus where it is connected and the loads are represented by DC-AC converters. Clearly, the DCT plays an important role in the DC PDN, connecting the DC buses and allowing the integration of renewable and storage systems in different voltages range. Further, as this system have dynamic loads and sources, the power flow changes according to them, which produces changes in power direction and potentially extreme conditions at the DCT branch. Nevertheless, for any situation, the DCT should be able to support the grid and enable the natural power flow between buses.

The DCT based on the resonant LLC converter has some special qualities that match the DC PDN requirements. To list a few: i) load-independent behavior when operating close to the resonant frequency; ii) ZVS is maintained for all the operating ranges, with quasi-ZCS with a constant current given by the magnetizing inductance, when operating slightly below

the resonant frequency; iii) galvanic isolation with MFT; and iv) bidirectional power transfer with simple implementation.

The resonant DCT under analysis is shown in Fig. 1b and 1c. The DCT is constructed as a symmetric LLC with split capacitors around the MFT. First, Fig. 1b shows a DCT with full bridge modules. This DCT, using unipolar PWM, has all the requirements to perform the essential features of the DCT (i.e. bidirectional operation and three-level operation). In this paper FBs power stages are used to test the methods due to the accessibility of LV equipment, which is sufficient to demonstrate the developed methods.

Nevertheless, developments of this work are aimed for the MV prototype, where IGCT NPC power stage in combination with split capacitor bank is used [12], [13], as shown in Fig. 1c. Results are not affected by the topology once the only aspect that matters are the square wave generation on the ac side, the capacity to create three-level for the transient, and bi-directionally.

III. DESCRIPTION OF THE ESSENTIAL FEATURES

The essential features of the DCT are the open-loop strategies that guide the converter's operation. As previously mentioned, the DCT does not require any closed-loop control for its operation, however, the operation modes need to be identified properly to ensure a safe operation. To start, the DCT is not switching, not processing any power, only waiting for the DC PDN to have a difference at the DC voltage levels, and then processing some power. Thus, the first operation mode consists of idle mode, when DCT is waiting for its criteria to be met and process some power.
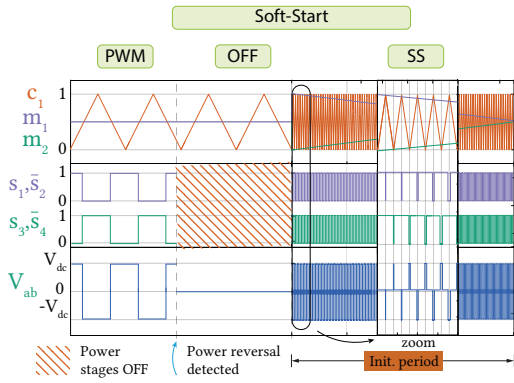
Fig. 2. Illustration of the PWM initialization sequence, and zoom-in on the three-level voltage in the resonant tank after power reversal. c_1 is PWM carrier, m_1 and m_2 are modulation indices for leg 1 and leg 2 respectively. s_x is the gate signal of device x, and V_{ab} is resonant tank voltage. After the DCT stops switching, the DCT starts operation with a three-level voltage waveform.

Further, some extra logic are required to allow its operation principles as; i) A soft-start strategy to avoid saturation of MFT and large inrush currents, and ii) power direction detection to determine the active power stage.

A. Soft-Start

Soft-start strategies for LLC converters are well-known and demonstrated in the literature. There are many methods already available [7], [14]–[16], and this paper adopts the duty cycle modulation, applied during every DCT start. This strategy is illustrated in Fig. 2. At first, the power stage is switching with both modulation indices of the unipolar PWM at 0.5. Then, the DCT turns off when a power reversal or no-load criteria is met, and modulates the indices to create a three-level voltage waveform when DCT is activated again.

During this transient (soft-start initialization period), the DCT is strongly non-linear and partly discontinuous behavior until the modulation indices return to 0.5. For that reason, one important feature of the soft start strategy for DCTs is the ability to change the soft-start time duration accordingly to the power demand [1]. This initialization period can be set by monitoring power or voltage, matching the system's dynamics, and improving the transient dynamics.

B. Idle Mode: No-load Operation

The no-load operation happens when the two DC buses have small difference in their respective voltage levels. During this period the DCT can stay idle, avoiding unnecessary power consumption on the MFT. Essentially, this mode defines when the DCT should turn ON and turn OFF.

Fig. 3 illustrates the Idle Mode operation principle. This logic checks the voltage difference, and after a certain hysteresis band, the DCT starts processing power or turns off. This mode also checks the rate of change of the voltage difference, in order to set the soft-start initialization period to match the system's dynamics.
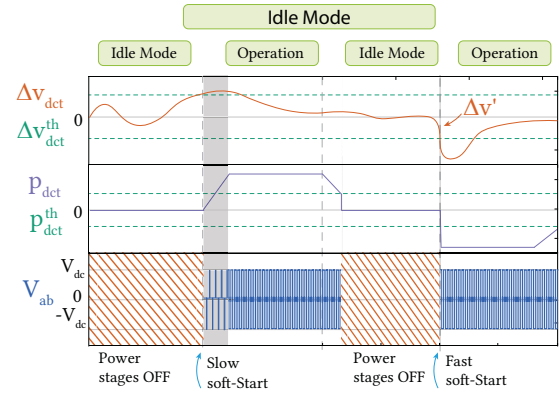

Fig. 3. Illustration of the idle Mode operation principle. The DCT is initialized only when the ΔV_{DCT} overcomes the voltage threshold ΔV_{DCY}^{th}. In case the voltage variation is fast, the soft-start duration period is reduced. At the moment the power processed by DCT is below the power threshold P_{th}, the DCT stops switching, reducing no-load losses. V_{ab} is the output voltage of power stages applied to the resonant tank.

In summary, with this strategy, the DCT will be activated once the expected power transfer is higher than the no-load losses of the MFT, with a soft start defined by the rate of change of the voltage difference. And, will deactivate the DCT once only magnetizing current in the MFT is flowing.

C. Power Reversal Strategy

The power reversal strategy is the logic that sets which power stage should be active to allow the natural power flow. In literature, there are several ways to identify the power direction. Some use the voltage gain and voltage measurements [17], [15], or resonant currents [18], or dc currents [1]. Any of these could be used to identify the power direction and properly issue the power reversal command for the DCT. This paper adopts the dc voltage measurements to determine the
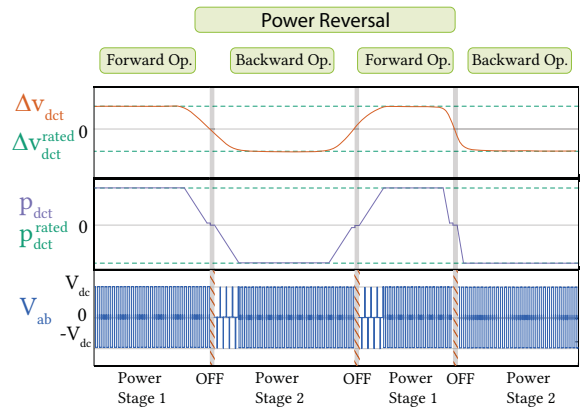

Fig. 4. Illustration of the Power Reversal logic. The DCT checks the voltage difference ΔV_{dct}. In case the voltage is positive the power direction is from one side, in case of a negative voltage difference, the power direction is the opposite. Soft-start is available in every power reversal.
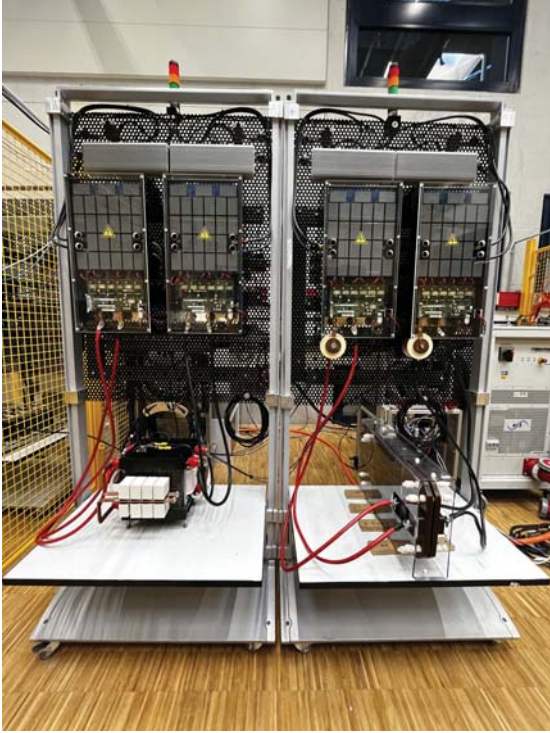
Fig. 5. Two DCTs prototypes side by side. Relays, charging circuit, controllers, and measurement units are on the back side of the panel.

power reversal as this is also used as criteria for the Idle Mode operation.

Fig. 4 illustrates the power reversal operation principle. The DCT checks the voltage difference between the two DC buses and verifies which direction the power should be flowing (from higher voltage to lower voltage.) Then, it outputs which power stage needs to be activated in order to allow the natural power flow of the system.

IV. EXPERIMENTAL VALIDATION

The aforementioned essential features were implemented and tested in two DCT prototypes developed in the laboratory. The DCT uses a three-phase VSI developed in the lab, with only two legs operated as FB. Figure 5 shows the two DCTs side by side. The power stages are controlled by ABB's AC 800PEC. The schematic of the complete system is shown in Fig. 6

The two DCTs have the same specifications with small differences in the resonant tank parameters. The DCT 1 (on the left side of Fig. 5) has a core type MFT made with square litz wire, air-insulated, core of SiFerrite (UU9316 - CF139) with air-cooled heatsink, and resonant capacitors mounted closely to the MFT [19]. While DCT 2 has a planar type MFT with windings made of copper and litz wire, nanocrystalline core (VITROPERM 500F), solid insulation (cast resin), and forced air for cooling, with external resonant capacitors [20]. The parameters of the DCTs are described in Table I.
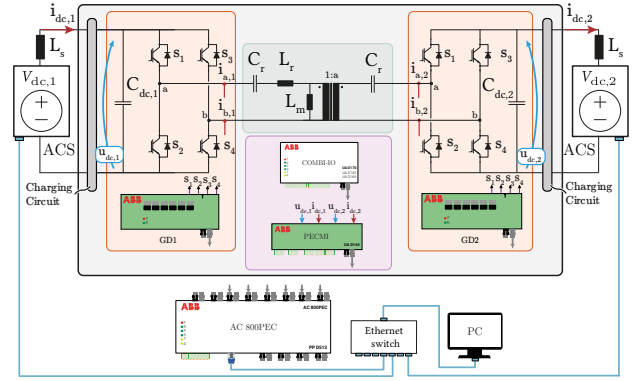

Fig. 6. Schematic of the complete system. The two DC buses are created with voltage sources. For the test setup system, the controller, relays, and power sources are accessed through PC.

TABLE I
EXPERIMENTAL SETUP PARAMETERS

Description	Symbol (Unit)	DCT 1	DCT 2
DC Voltage 1	$V_{dc,1}$ (V)	750	
DC Voltage 2	$V_{dc,1}$ (V)	750	
Rated power	P_n (kW)	50	
Grid inductance	L_s (μH)	30	
Grid resistance	R_s (Ω)	0.1	
Turns ratio	$1 : a$	1:1	
Switching frequency	f_{sw} (kHz)	10	
Leakage inductance	L_r (μH)	11.6	9.5
Magnetizing inductance	L_m (μH)	750	1100
Resonant capacitor	C_r (μH)	37.5^a	37^b
Line resistance	R_c (Ω)	0.1	0.1

^{a} $\pm 5\%$ tolerance, ^{b} $\pm 10\%$ tolerance

Fig. 7 shows the schematic of the DCTs and the power transfer characteristics for both DCTs, from the modeling and experiments. The voltage gain characteristic is the relationship between the voltage gain and the transferred power. In this figure, the voltage gain is defined as $V_{dc,2}/V_{dc,1}$, and positive power transfer is from power stage 1 to power stage 2. In this sense, both DCTs have similar characteristics, and it can be noticed that differences of 10 V can lead to approximately 25 kW for DCT 1 and 30 kW for DCT 2.

A. Experimental results

The experimental setup consists of two energized DC buses from ACS, and the DCT with the charging resistors proceeds with the start-up sequence. First, the capacitors of DCT are charged through charging resistors which are further bypassed. Then, to simulate any load variation, the voltages of the two DC buses are modulated in order to provoke various power flows.

For all the experiments, the DC bus 1 was regulated to $V_{DC,1} = 750\ V$, while the DC bus 2 varies following the emulated load dynamic. Firstly, in order to provoke a power flow around $P_{DC} \approx 40$ kW, the DC bus 2 is set to $V_{DC,2} = 734\ V$. Figure 8 shows the experimental results for the resonant currents and voltages. On top is the forward
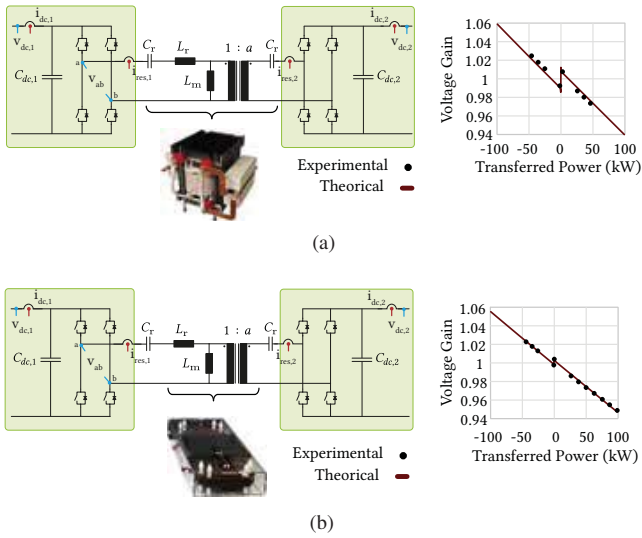
Fig. 7. Power transfer characteristic of the two DCT prototypes with experimental data. (a) DCT 1 and (b) DCT 2. The voltage gain is $V_{dc,2}/V_{dc,1}$.
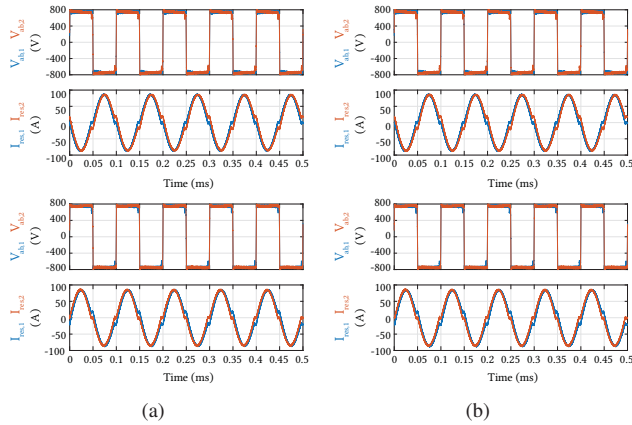

Fig. 8. Experimental waveform of the two DCTs operating with 40kW for forward (top) and backward (bottom) operation. In (a) the waveforms from DCT 1, and in (b) for DCT 2.
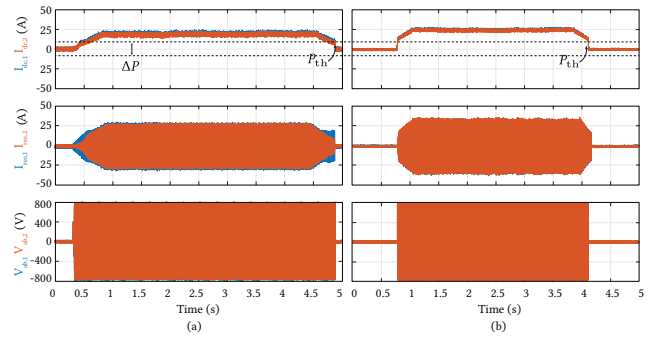

Fig. 9. Experimental waveforms showing the DCT in Idling Mode, with a Power threshold. The DCT operates only during the period when a load is requested. In (a) waveforms of DCT 1 and in (b) for DCT 2.
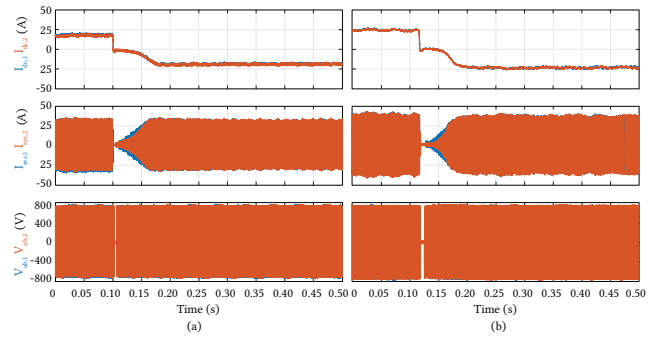

Fig. 10. Experimental waveforms showing the DCT power reversal transient for a step change. The forward and backward operation processing $P_{DC} \approx 18$ kW is shown for (i) DCT 1 and (ii) DCT 2. During power reversal, the DCT stops during a small period of time in Idle mode, and reverses the power with soft-start as soon as the criteria to start the operation is met.

operation and on the bottom the backward operation. The DCT 1 has a turn-off current of around 22 A, while DCT 2 has a turn-off current of around 17 A.

Now, in order to test the idle mode logic, the DC bus 2 is set to $V_{DC,2} = 742$ V, for both DCTs and experimental waveforms are shown in 9. For this experiment, the threshold to start its operation was set to $V_{th} = 4$V and the power threshold was set to be $P_{th} = 1.5$ kW for both DCTs. First, the experiment starts with both DC buses regulated to 750 V. Then, the load starts increasing slowly with a slope of $dv/dt = 0.025$ V/ms. When the DCT notices a difference of 4 V, the DCT starts operation with soft-start and feed the load. Later, the load decreases, and as soon the DCT note that the processed power is below the threshold it turns off.

As the pre-set threshold values were fine-tuned for DCT 1, it can be seen that DCT 2 have slightly different behavior for this load profile. Both DCTs face the same voltage difference, but DCT 2 allows a bit more current throughout its branch. Also, when the load reduces, the power threshold is a bit high for DCT 2, and the DCT turns off while still having a small current being transferred. In this sense, this highlights the importance of fine-tuning the threshold parameters for each DCT.

Now, Fig. 8 shows the experimental results for the power reversal logic. The load step is performed, changing $V_{DC,2} = 742$ V to $V_{DC,2} = 755$ V with a slope of $dv/dt = 5$ V/μs. In this experiment, the DCT is feeding a load with forward operating mode, and suddenly, the load change inverting the power flow. As expected both DCT have similar behavior for the same step change. In both cases, the load first goes to zero, then for a short period, the DCT is in Idle Mode until the criteria to start the operation is met again. As soon as the voltage difference is met the DCT starts processing power to the other side.

B. Parallel Operation of DCTs

The obvious advantage of the parallel operation is the possibility to increase the power rating to meet the demands of higher power applications. With this configuration, the scalability of DCT is enlarged while keeping the same operational
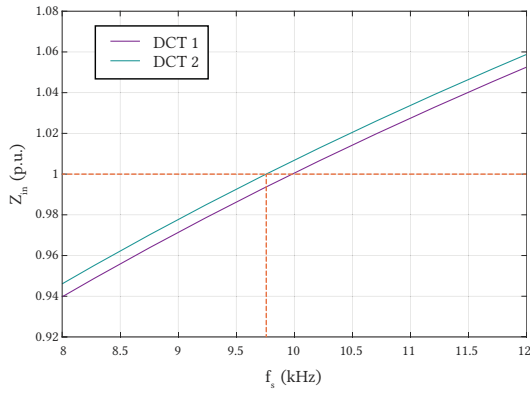
Fig. 11. Variation of the input impedance of the experimental DCT for different switching frequencies. The dashed orange line highlights the same input impedance value and the respective switching frequency that DCT 2 should operate for perfect current sharing.
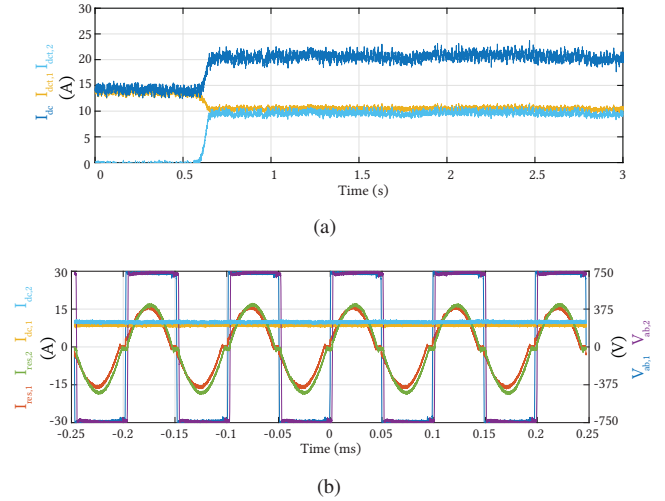

(a)

(b)

Fig. 12. Experimental waveform of the parallel operation of 2 DCTs operating at 10 kHz. (a) DC current of each DCT and total DC current; (b) Details on the resonant currents on the secondary, voltage applied to the resonant tank, and the dc current of each DCT. Numbers 1 and 2 represent DCT 1 and DCT 2 respectively.

principle of a single unit. However, as every parallel module is slightly different, there is a natural unbalance on the current sharing between modules.

The current sharing in steady-state is given by the input impedance of each DCT, which is very sensitive to resonant tank parameters and to the switching frequency. Therefore, by knowing that, the current sharing unbalance can be corrected by changing the switching frequency. The input impedance of the two DCTs for different switching frequencies is shown in Fig. 11. Then, if necessary, the switching frequency could be used to enhance the current sharing performance. As an example, to reach perfect current sharing with the two prototypes, the horizontal line highlights the same impedance point for both DCTs. In this case, with DCT 1 operating at 10 kHz, DCT 2 should operate at 9.75 kHz to have the same impedance value, and therefore, share the load perfectly.

The parallel operation of the two prototypes is shown in Fig. 12. The experiment proceeds as follows: i) DCT 1 starts its operation and transmits the power according to the voltage difference of the two DC ports; ii) DCT 2 is enabled and DCTs start sharing the current naturally. The PWM signals are not synchronized. Fig. 12a shows the experimental waveforms of the DC currents, and Fig. 12b shows details of the resonant currents, the voltage applied to the resonant tank, and the DC current of each DCT. In particular, due to the construction of the prototype, both have very similar input impedance and have good current sharing, with $I_{DCT,1} \approx 11$ A, and $I_{DCT,2} \approx 10$ A.

V. AUTONOMOUS OPERATION

The autonomous operation of the DCT consists in creating a set of pre-defined thresholds and rules which guide the DCT through its operation. These rules depend strongly on the development philosophy and the application. For DCT in DC PDN, ideally the DCT should be left to operate alone similarly to the AC transformer. Still, a controller is needed to set the previously discussed open-loop strategies and
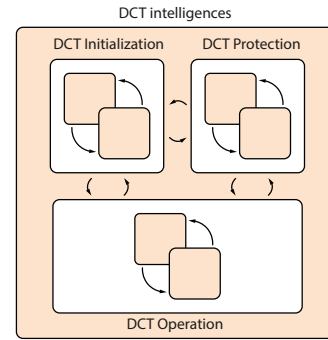

Fig. 13. Interconnection of the state machines to coordinate autonomous operation of the DCT.

command PWM signals for the switches. As an example, Fig. 13 shows an overview of the complete state machine for DCT operation with three main inner blocks: DCT Initialization, DCT Protection, and DCT Operation.

For each inner state machine, different logic could be implemented as described as follows:

- DCT Initialization: Responsible for controlling relays, charging DC links, and issuing operational flags. It has the slowest update rate.
- DCT Protection: Responsible for setting the protection logic and issuing protection flags. It needs to have faster update rate.
- DCT Operation: Responsible for all the operation open loop strategies as soft-start, power reversal, idle mode, PWM, etc. This is susceptible to protection flags and requires operational flags from other blocks. It does not require the same update rate as protection, but it depends on how fast the measurements are processed.

Thus, as no set point is required for any of these open loop control logic, the DCT can operate alone, without an external agent. This contributes to creating a DCT acting as close as possible to the AC transformer.

VI. CONCLUSION

The DCT based on the resonant LLC converter has great characteristics to be the dc-dc converter to allow more advanced dc power distribution networks. In order to allow its open loop operation, the essential features described in this paper need to be implemented to perform a safe and reliable operation.

All the presented features consist in simple open-loop strategies to allow the DCT to follow the natural system's dynamics. The demonstration of the developed methods in two DCTs with similar characteristics showed how they perform, and highlighted the importance of a proper fine-tuning of threshold values for an optimal operation.

REFERENCES

[1] R. P. Barcelos, J. Kucka, and D. Dujic, "Power reversal algorithm for resonant direct current transformers for dc networks," *IEEE Access*, vol. 10, pp. 127 117–127 127, 2022.

[2] X. Xie, J. Zhang, C. Zhao, Z. Zhao, and Z. Qian, "Analysis and optimization of llc resonant converter with a novel over-current protection circuit," *IEEE Transactions on Power Electronics*, vol. 22, no. 2, pp. 435–443, 2007.

[3] B. Yang, F. Lee, and M. Concannon, "Over current protection methods for llc resonant converter," in *Eighteenth Annual IEEE Applied Power Electronics Conference and Exposition, 2003. APEC '03.*, vol. 2, 2003, pp. 605–609 vol.2.

[4] W. Sun, X. Jin, L. Zhang, H. Hu, and Y. Xing, "Analysis and design of a multi-resonant converter with a wide output voltage range for ev charger applications," *Journal of Power Electronics*, vol. 17, pp. 849–859, 2017.

[5] S. Liu, R. Ren, W. Meng, X. Zheng, F. Zhang, and L. Xiao, "Short-circuit current control strategy for full-bridge llc converter," in *2014 IEEE Energy Conversion Congress and Exposition (ECCE)*, 2014, pp. 3496–3503.

[6] D. Yang, C. Chen, S. Duan, J. Cai, and L. Xiao, "A variable duty cycle soft startup strategy for llc series resonant converter based on optimal current-limiting curve," *IEEE Transactions on Power Electronics*, vol. 31, no. 11, pp. 7996–8006, 2016.

[7] Q. Chen, J. Wang, Y. Ji, and S. Liang, "Soft starting strategy of bidirectional llc resonant dc-dc transformer based on phase-shift control," in *2014 9th IEEE Conference on Industrial Electronics and Applications*, 2014, pp. 318–322.

[8] H. Bishnoi, S. Alvarez, G. Ortiz, and F. Canales, "Comparison of overload protection methods for llc resonant converters in mvdc applications," in *2018 IEEE Energy Conversion Congress and Exposition (ECCE)*, 2018, pp. 3579–3586.

[9] J. Kucka and D. Dujic, "Current limiting in overload conditions of an llc-converter-based dc transformer," *IEEE Transactions on Power Electronics*, vol. 36, no. 9, pp. 10 660–10 672, 2021.

[10] J.-W. Kim, M.-H. Park, B.-H. Lee, and J.-S. Lai, "Analysis and design of llc converter considering output voltage regulation under no-load condition," *IEEE Transactions on Power Electronics*, vol. 35, no. 1, pp. 522–534, 2020.

[11] C. Fei, Q. Li, and F. C. Lee, "Digital implementation of light-load efficiency improvement for high-frequency llc converters with simplified optimal trajectory control," *IEEE Journal of Emerging and Selected Topics in Power Electronics*, vol. 6, no. 4, pp. 1850–1859, 2018.

[12] G. Ulissi, U. R. Vemulapati, T. Stiasny, and D. Dujic, "High-frequency operation of series-connected igcts for resonant converters," *IEEE Transactions on Power Electronics*, vol. 37, pp. 5664–5674, 5 2022.

[13] N. Djekanovic and D. Dujic, "Copper pipes as medium frequency transformer windings," *IEEE Access*, vol. 10, pp. 109 431–109 445, 2022.

[14] J. Sun, L. Yuan, Q. Gu, and Z. Zhao, "Startup strategy with constant peak transformer current for solid-state transformer in distribution network," *IEEE Transactions on Industry Applications*, vol. 55, no. 2, pp. 1740–1751, 2019.

[15] J. H. Jung, H. S. Kim, M. H. Ryu, and J. W. Baek, "Design methodology of bidirectional cllc resonant converter for high-frequency isolation of dc distribution systems," *IEEE Transactions on Power Electronics*, vol. 28, pp. 1741–1755, 4 2013.

[16] J. Sun, L. Yuan, Q. Gu, and Z. Zhao, "Startup strategy with constant peak transformer current for solid-state transformer in distribution network," *IEEE Transactions on Industry Applications*, vol. 55, no. 2, pp. 1740–1751, 2019.

[17] J. M. Burdío, L. A. Barragán, F. Monterde, D. Navarro, and J. Acero, "Asymmetrical voltage-cancellation control for full-bridge series resonant inverters," *IEEE Transactions on Power Electronics*, vol. 19, pp. 461–469, 3 2004.

[18] J. Kucka and D. Dujic, "Smooth power direction transition of a bidirectional llc resonant converter for dc transformer applications," *IEEE Transactions on Power Electronics*, vol. 36, no. 6, pp. 6265–6275, 2021.

[19] M. Mogorovic and D. Dujic, "100 kW, 10 kHz medium-frequency transformer design optimization and experimental verification," *IEEE Transactions on Power Electronics*, vol. 34, pp. 1696–1708, 2 2019.

[20] D. Dujic, J. Kucka, G. Ulissi, N. Djekanovic, and R. Barcelos, "Bulk dc-dc conversion for mvdc applications," *TUTORIAL at: EPE'22 ECCE Europe, European Conference on Power Electronics and Applications, Hannover, Germany, September, 5-9, 2022*, 2022. [Online]. Available: http://infoscience.epfl.ch/record/296466